MIR spectral characterization of plastic to enable discrimination in an industrial recycling context: III. Anticipating impacts of ageing on identification

Charles Signoret [a], Marie Edo [a], Anne-Sophie Caro-Bretelle [b], José-Marie Lopez-Cuesta [a], Patrick Ienny [b], Didier Perrin [a,*]

[a] *Polymers Composites and Hybrids (PCH), IMT Mines Ales, France*
[b] *LMGC, IMT Mines Ales, Univ Montpellier, CNRS, France*

A B S T R A C T

Ageing of polymers entails important structural changes and degrades their functional properties, particularly their aspect. Since sorting is a primordial step in recycling to achieve acceptable mechanical properties, the use of promising technologies such as MIR-HSI (Mid-Infrared Hyperspectral Imagery), which could overcome black plastics sorting issue, has to take into account the influence of ageing on identification. As ageing strongly impacts spectra, it can create confusion between materials, especially in an automatized scheme.

Based on laboratory FTIR-ATR (Fourier-Transform Infrared Attenuated Total Reflection), this work investigates spectral evolutions of natural and accelerated photodegradation of Waste of Electric and Electrical Equipment plastics (WEEE) as PE, PP, HIPS, ABS and PC to help identifying a polymer despite its ageing degree. Oxidation marks were described and retrieved within a stock of about one hundred of real waste samples, then differentiated from other sources of spectral alteration as formulation.

Laboratory ageing data were found to be consistent and often more extreme than real waste samples values. Generally, styrenics showed stronger spectral alteration than polyolefins despite their respective aspects. No significant spectral alteration of PC was obtained here or observed in the waste stock. As an important oxidation marker, the carbonyl peak was also found to often enable fast identification through its wavenumber. If well taken in account, ageing should not induce confusion with other polymers, even formulated, as characteristic signals are different. Finally, the different industrial sub-ranges within MIR are not affected at the same degree, possibly influencing a technological choice for industrial sorting.

Keywords:
Polymer recycling
MIR
Identification
Photooxidation
Infrared spectroscopy
Plastic waste

1. Introduction

Because of their easy processing, low density, affordable costs and interesting range of properties, plastics are widely distributed and often rapidly discarded as worthless waste (Thompson et al., 2009). Described as "a fantastic" material in the past which would revolutionize the world (Yarsley and Couzens, 1941), it presents several ecological benefits: it can limit food waste (Silvenius et al., 2014); it can lighten structures and diminish associated carbon dioxide emissions (Akhshik et al., 2019); moreover, it is less energy demanding than other materials, as metal or glass, in its production and transformation. However, the image of plastic is nowadays strongly deteriorated by its strong dissemination in the environment (Andrady, 2017; Brennecke et al., 2016; Gall and Thompson, 2015; Gallo et al., 2018; Kedzierski et al., 2018;

Abbreviations: ABS, Acrylonitrile Butadiene Styrene; Acc, Accelerated ageing (QUV); ASA, Acrylonitrile Styrene Acrylate; ATR, Attenuated Total Reflection; EVA, Ethylene Vinyl Acetate; FTIR, Fourier Transform Infrared; HDPE, High Density Polyethylene; HIPS, High Impact Polystyrene; HSI, Hyperspectral Imagery; LIBS or LIPS, Laser Induced Breakdown/Plasma Spectroscopy; LDPE, Low Density Polyethylene; LWIR, Long Wavelength Infrared (7.4–14.0 μm or 1350–700 cm^{-1}); MFI, Melt Flow Index; MIR, Mid-Infrared (4000–400 cm^{-1} or 2.5–25.0 μm); MWIR, Middle Wavelength Infrared – 2 to 5 μm (5000 to 2000 cm^{-1}); Nat, Natural ageing; **NIR**, Near-Infrared – 0,8 to 2,5 μm (12500 to 4000 cm^{-1}); PA, Polyamides; PC, Polycarbonate (from bisphenol A); PE, Polyethylene (HDPE or LDPE); PET, Polyethylene terephthalate; PLA, Polylactic acid; PMMA, Polymethylmethacrylate; PP, Polypropylene; PPC, Polypropylene copolymer; PPH, Polypropylene homopolymer; PS, Polystyrene; PU, Polyurethanes; TPU, Thermoplastic PU; UV, Ultraviolet; WEEE, Waste of Electrical & Electronic Equipment; γ, out-of-plane deformation; δ, in-plane deformation; ν, stretching.

* Corresponding author.
E-mail address: didier.perrin@mines-ales.fr (D. Perrin).

Rahmani et al., 2018). With reduction at source and reuse to valorize at most already produced goods, a proper disposal of plastic waste is thus a strong subject of interest.

The first obstacle to plastics durability and recycling is their nature itself. As organic materials, they are strongly subjected to oxidation (Celina, 2013). Limited by oxygen diffusion and/or UV light penetration, ageing is often confined to the surface (Collin et al., 2012). However, it is sufficient to strongly depreciate aspect properties, mainly through an infamous yellowing which results of the formation of conjugated species. PC (polycarbonate) important yellowing was thus finely described through the photo-Fries mechanism which modifies carbonates functions between aromatic cycles into hydroxyls and ketones directly on the cycles, thus generating discoloration since they are conjugated (Rivaton, 1995). Jouan et Gardette (Jouan and Gardette, 1992) demonstrated corresponding mechanisms for styrenics by highlighting a chromophore issued from chain scission of polystyrene segments. More generally, Gardette et al. (Gardette et al., 1995) described principal mechanisms of styrenic photooxidation where hydroperoxides decomposition leads to many reactions paths where carbonyl apparition often corresponds to chain scission and volatiles formation. These carbonyls take many forms: lactones, ketones, aldehydes, carboxylic acids... However, hydroxyl production rapidly ends hydroperoxides rich reactivity, hampering the apparition of many oxidized species and chain scission. Moreover, they highlighted that polybutadiene (PB), which differentiate brittle styrenics, GPPS (General Purpose Polystyrene) and SAN (Styrene-Acrylonitrile), from impact-modified ones, HIPS (High Impact Polystyrene) and ABS (Acrylonitrile-Butadiene-Styrene), is the prime target of photo-oxidation, also confirmed by several authors (Boldizar and Möller, 2003; Shimada and Kabuki, 1968; Vilaplana et al., 2011), and even initiates the matrix degradation. Our research group (Signoret et al., n.d) found a strong negative interaction between primary photodegradation and recycling of impact-modified styrenics, which induced important material discoloration and loss of impact properties. Especially, surface oxidation induced bulk modifications after reprocessing. It could be thus advisable to segregate too oxidized material or to restabilize it accordingly. Consequently, it is important to recognized an aged material as such.

Devoid of any unsaturation, polyolefins are thus less impacted by discoloration but other aspect properties can also be deteriorated, especially gloss and transparency (Song et al., 2014). This can be explained, in the case of important chain scissions, by chemicrystallization which also induces cracks formation because of shrinkage (Rabello and White, 1997). Similarly to styrenics, chain scissions within polyolefins are expressed through many carbonyl-based species whereas crosslinking is described by Chabira et al. (Chabira et al., 2012) as a simple recombination of chain radicals, generating C-C bonds. Consequently, this mechanism is fostered by the presence of tertiary alkyls, more stable and then having a chance to react, thus in LDPE (Low Density Polyethylene) compared to HDPE (High Density Polyethylene) (Chabira et al., 2012). Luzuriaga et al. (Luzuriaga et al., 2006) found, especially through DSC (Differential Calorimetry Index) and MFI (Melt Flow Index) measures, that PP is more prone to chain scissions, contrary to PE, more prone to crosslinking. They explained this difference by measuring hydroperoxide contents through spectrocolorimetry. They found that hydroperoxide formation was very strong in PP (Polypropylene), but not in PE, especially HDPE, which can be explained by the low stability of secondary alkyl radicals. Similarly with what they did with styrenics, Gardette et al. (Gardette et al., 2013) described the formation of several carbonyl species through photooxidation of PE, which here also develops important Norrish I and Norrish II reactivity. These chain ketones reactions to UV generate even more chain scission and Norrish II is highlighted by methylketones and end-of-chain vinyls formation. Methylketones then further reacts to create vinyls and acetone.

With ageing, the second strong obstacle to recycling is the variety of commercialized plastics without even considering the numerous grades and formulations proposed on the market. Sadly, most of polymer types are incompatible, meaning that their recycling in mixes leads to very poor properties (Maris et al., 2018; Ragaert et al., 2017). Industrial separation is thus mandatory to render recycled plastics economically pertinent (Gundupalli et al., 2017; Vrancken et al., 2017). Nowadays, NIR HSI (Near-Infrared Hyperspectral Imagery), the main technology which enables industrial polymer separation of complex stocks, is limited by the use of carbon black as a pigment (Beigbeder et al., 2013) which is intensively present in WEEE (Waste of Electrical and Electronic Equipment) and ELV (End-of-Life Vehicles). Several other technologies exist but ageing could negatively impact them since a lot of them mainly work on surface. Froth flotation (Wang et al., 2015) or triboelectrostatic separations (Wu et al., 2013), based on surface tensions, could be impacted by surface oxidation. Optical technologies, as NIR (Alassali et al., 2018), well established, LIBS (Laser Induced Breakdown Spectroscopy) (Grégoire et al., 2011; Roh et al., 2018), Raman (Bae et al., 2019; Roh et al., 2017) or MIR (Mid-Infrared) (Kassouf et al., 2014; Rozenstein et al., 2017; Signoret et al., 2019a), are surface analysis and thus can be impacted, especially as surface chemistry can be deeply changed as reported above from the literature. Moreover, industrial identification is currently made in degraded conditions in comparison to laboratory analysis. Obtained data are restricted, of diminished resolution, with a strong noise and must be done at high speed to enable the sorting operation. Thus, the use of classification algorithms can be of great help to achieve industrial separation (Bae et al., 2019; Oh et al., 2014; Roh et al., 2018, 2017). The choice and comprehension of training data is determinant in a successful classifier construction. Incorporating controlled aged samples is then interesting, especially to prevent recognizing an aged polymer as another one. Here these modifications are described at laboratory to anticipate possible impacts of ageing on identification.

The two previous works focused on the identification of specific patterns of respectively styrenics polymers and their blends (Signoret et al., 2019a), and polyolefins and chemically close polymers (Signoret et al., 2019b). The goal of this study is to specifically recognize ageing patterns in MIR (Mid-Infrared) and highlight possible confusions with other plastics, especially formulated ones. This aims both to recognize a polymer despite its ageing, or to specifically identifying it as aged in the case of segregation is considered as preferable. Finally, this study can be seen as a help to both industrial sorting and laboratory identification. FTIR (Fourier-Transform Infrared), working in MIR, is the most recurring technique to monitor polymer ageing and important distortions are showed. However, an important part of the literature only displays very specific ranges, which are characteristic of polymer ageing (O—H, C=O, C—O...), and focus on a few polymer natures if not only one, without comparing it to real waste samples. The present study considers the whole MIR range, from 4000 to 400 cm^{-1} with identification sustainability as primary objective. Thus comparisons between polymer natures and to waste samples are here primordial. Current associated industrial technology, namely hyperspectral imagery (HSI), covers two ranges within MIR: MWIR, mid-wavelength infrared defined from 5000 to 2000 cm^{-1} (2–5 μm) and LWIR, long-wavelength infrared, roughly from 1350 to 700 cm^{-1} at maximum (7.4–14.0 μm) even if commercial LWIR ranges tend to vary.

In this purpose, natural and accelerated ageing were applied to virgin samples of LDPE, polypropylene homopolymer (PPH), GPPS, HIPS, SAN, ABS, acrylonitrile-butadiene-acrylate rubber (ASA) and PC. Comparisons were made between ageing modes and between

pristine commercial samples and samples from real waste of municipal deposits and WEEE deposits (Waste of electric and electrical equipment) for styrenics in MWIR and LWIR, and then specific polyolefin collection. As an important ageing marker but also a specific signal for several virgin polymers (PMMA, PET, PA...), a focus was also made on the carbonyl peak in the last part of this study, even if it is currently off-range for MWIR and LWIR.

2. Materials and methods

2.1. Materials

Table 1 displays used polymer references during this study:

Two samples of the Matériautech (Allizé-Plasturgie, n.d.) were used as spectral references: PLA (PLI 004 from Natureplast) and PET (Multiflex SIE s 7007 SPA1 NAT, Multibase). 112 plastic waste samples were also supplied by the Suez Company from their waste processing plants in Berville-sur-Seine (NORVAL) and Feyzin (SITA) in France. About a third was from screen casings. Waste stocks were mainly WEEE but also issued from the sinking fraction of municipal deposits. Most of these samples were unable to be identified with NIR-HIS as they were rather dark-coloured. Within this stock, 20 were identified as PP, 5 as PE, 1 as PEX, 12 as PVC, 1 as PE/PVC, 3 as POM, 9 as ABS, 32 as HIPS, 7 as HIPS/PPO, 6 as ABS/PC, 1 as ABS/PVC, 2 as ABS/PMMA, 2 as PMMA, 1 as PMMA/PC, 3 as EVA, 3 as PA, 1 as PET and 3 as PC.

2.2. Sample preparation

Polymer plates ($100 \times 100 \times 4$ mm^3) were injected thanks to a Kraus-Maffei 180/CX 50 molding injection press at 230 °C and molded at 40 °C with internal mold pressure maintained at 300 bars for 12 s then 275 for 12 other seconds between injection cycles. Styrenics (GPPS, HIPS, SAN, ASA and ABS) were dried for 16 h at 80 °C before processing.

2.3. Ageing conditions

Natural ageing was realized in Alès (France, 44°08′09.0″N 4°05′54.3″E) from the beginning of April to the end of July 2018 on metallic racks shown on Fig. 1**.** They are inclined at 45°, directly exposed to the South. Exposed polymer plates were $4 \times 100 \times 100$ mm^3. Weather conditions, namely temperature and relative humidity, were monitored and presented in another work (Signoret et al., n.d). Temperature averages steadily rose from 20 °C to 30 °C at the end of tests, with roughly ± 10 °C variations around these values to reach minimal and maximal temperatures. Average humidity was measured at 60%. Plates were removed less than one hour each time for FTIR-ATR analysis. As seen on Figs. 1, 10 plates were put to age for LDPE, PPC, ABS, HIPS and PC but only two for ASA, SAN and GPPS.

Accelerated ageing was performed in a Q-UV tester (Q-Lab ("QUV Accelerated Weathering Tester," n.d.)) shown on Fig. 2. Weathering cycles were conducted at 65 °C, no humidity conditions and UV-A irradiation at 0.76 W/m^2. Because of space limitation, tests were made on roughly $4 \times 10 \times 100$ mm^3 rectangles cut from plates. As for natural ageing, samples were removed less than one hour for analysis. 3 samples were put for all materials except for ASA, GPPS and SAN.

2.4. FTIR-ATR spectroscopy

A Vertex 70 FT MIR spectrometer from Bruker with an ATR unit was used. The used resolution was 4 cm^{-1}, 16 scans for background acquisition and 16 scans for the sample spectrum. Spectra were acquired from 4000 to 400 cm^{-1}. All samples were cleaned with ethanol and dried. At least three measures were done for each material and ageing duration until two similar spectra were found with satisfying quality. One of these spectra were then chosen for further processing. Spectra were processed thanks to Matlab 2018 and plotted with Origin 9. FTIR-ATR (Attenuated Total Reflection) was chosen for convenience and to be closer to HSI cameras as both technologies are reflective.

2.5. Spectra comparison methodology description

The methodology used in this series of works lies on the use of charts as Table 1. It gathers every significant observed signal within a wavelength range. Each column corresponds to a 10 cm^{-1} wide (to anticipate low resolution) range where a signal was observed on a sample. Thus, two adjacent columns are not necessarily adjacent in values. Colors relate relative intensities within a range, from purple for exceptionally strong signals to pale yellow for hardly noticeable peaks. If exhaustive enough, these charts rapidly enable to identify important signals in identification and, in the other way, give one or several suspects for an unknown encountered peak. MWIR and LWIR charts are available in *supporting information* as well as well full MIR (4000–400 cm^{-1}) spectra as discussion below focus on MWIR, on extended LWIR, then on carbonyl area. The two first tables describe the ageing of polyolefins, styrenics and PC in a similar way as Table 2. Representing the outcome of the whole works series, the two second ones summarize signals of virgin polyolefins, PVC, POM, styrenics, PLA, polyesters, polyamides and PU, but also additives, cellulosic materials and atmospheric species (water and carbon dioxide).

3. Results and discussion

3.1. Styrenics: HIPS & ABS

3.1.1. Ageing of pristine references

Styrenics went through more or less severe color changes depending on nature and ageing type (Signoret et al., n.d). Whereas spectra of simple matrices, GPPS and SAN, did not visibly evolve (Fig. 3), polybutadiene-reinforced counterparts, HIPS and ABS, show oxidation marks through two convoluted bumps from 3000 to 3700 cm^{-1}, and from 2200, associated to O—H stretching of, respectively, simple alcohol functions (dark blue) and carboxylic acids (pink), confirming PB role in photo-oxidation (Gardette et al., 1995; Shimada and Kabuki, 1968; Vilaplana et al., 2011). ASA is an alternative to ABS for outdoor applications as its elas-

Table 1
List of polymer references used during this study.

Polymer	LDPE	PPH	GPPS	HIPS	SAN	ABS	ASA	PC	PMMA	PA6	TPU
Commer-cial name	2100NT00	PPH 9020	PS crystal 1340	Polystyrol 485 I	Luran 388 S	Terluran GP-35	Luran S 757G	Makrolon 2805	Altuglas V825T	Technyl C 206	IrograngA90P 5055
Company	LG Chem	Total	Total	BASF	Styro-lution	BASF	Styro-lution	Bayer	Arkema	Solvay	Huntsman

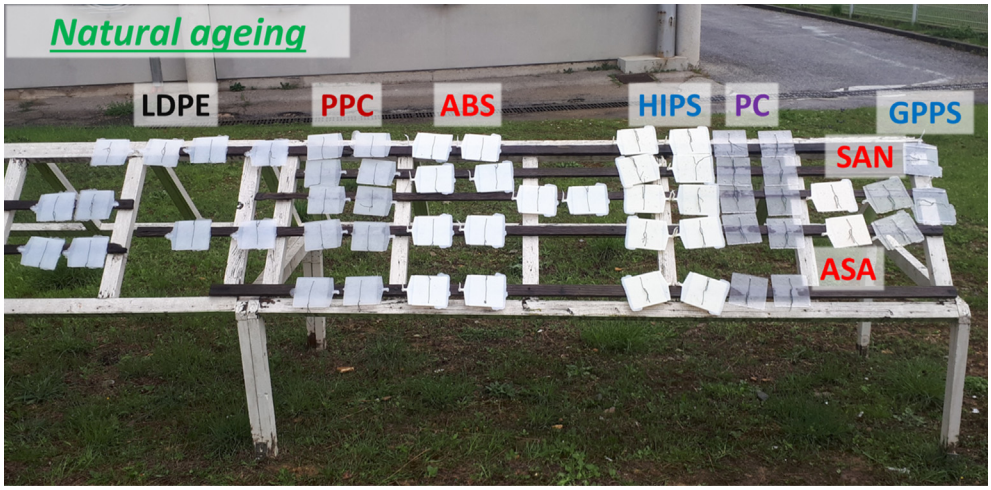

Fig. 1. Polymer plates submitted to natural weathering on wooden racks in Alès, France.

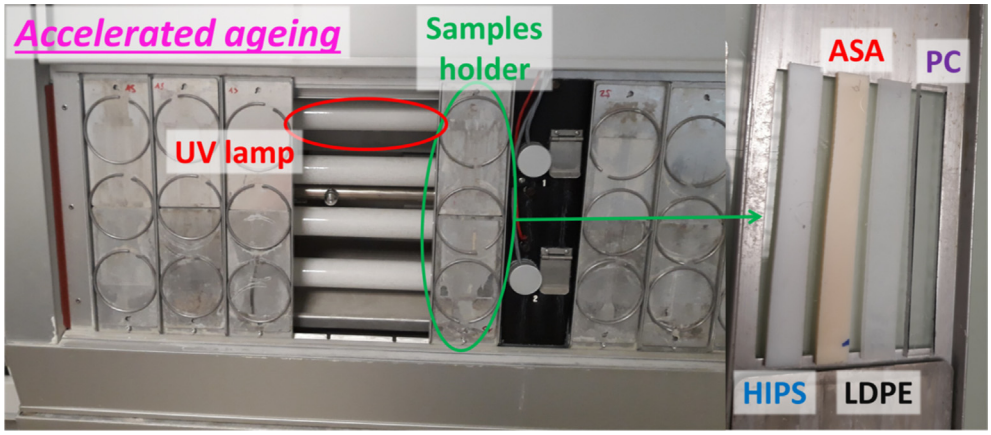

Fig. 2. Q-UV tester for accelerated weathering on rectangular polymer samples – red circle for UV lamp, green circle for sample holder – example of HIPS, ASA, LDPE and PC samples.

Table 2
MWIR styrenics specific signals before/after ageing – yellow–red colors correspond to relative intensities.

	Ageing	3700	3300	3080	3060	3025	3000	2955	2930	2920	2870	2850	2240	2000
GPPS	Virgin			3081	3059	3025	3002			2920		2849		
	Nat&Acc	max ≈ 3400												
HIPS	Virgin			3081	3059	3025	3002			2920		2849		
	Acc	engulf characteristic peaks												
	Nat	max ≈ 3300												
SAN	Virgin			3083	3061	3026	3003			2923		2854	2237	
	Nat&Acc													
ASA	Virgin			3085	3060	3027	3003	2957	2929		2874		2237	
	Nat&Acc	max ≈ 3400												
ABS	Virgin			3083	3061	3026	3003			2921		2851	2237	
	Acc	max ≈ 3300												
	Nat	max ≈ 3300												

tomeric phase, butyl acrylate rubber, is more resistant to ageing (Du et al., 2012) as Fig. 3 corroborates. However, ASA is still more sensitive to oxidation than SAN alone, as O—H groups appear.

Relative ratios between the two hydroxyl bumps demonstrate that, in accelerated conditions, alcohol formation is favored in ABS compared to HIPS. However, naturally aged samples are comparable

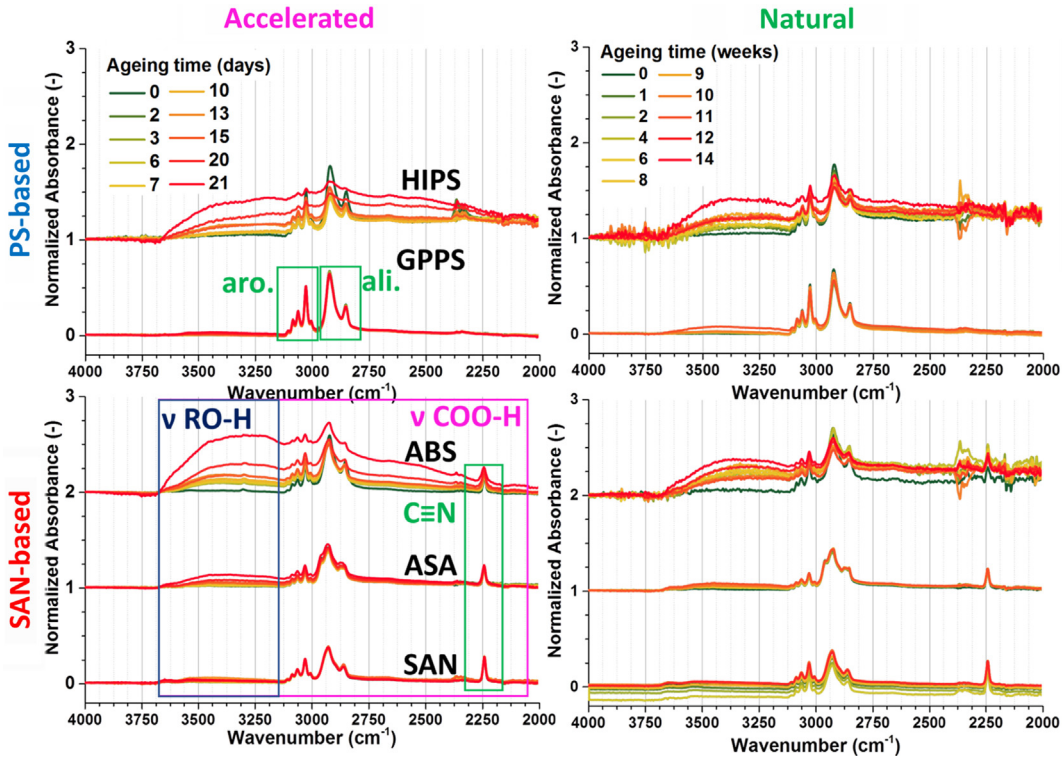

Fig. 3. FTIR-ATR spectra of styrenics aged in both accelerated and natural conditions – MWIR range – spectra normalized on the 1452 cm^{-1} peak height – green frame for characteristic signals of styrenics, blue frame for alcohol functions and pink frame for acids.

with rather little occurrence of acids. Whereas alcohols do not interfere much which identification, partially masking the aromatic C—H stretching weak peaks from 3000 to 3200 cm^{-1}, carboxylic acids can be very detrimental. Especially with artificially aged HIPS, aliphatic C—H stretching peaks at 2915 and 2850 cm^{-1} become less and less visible. ABS very characteristic nitrile peak at 2235 cm^{-1} is less impacted as it is aside, but its detection could be troublesome with diminished acquisition parameters. However, corresponding naturally aged materials are less impacted, as features are weaker and mainly associated to simple alcohols.

Fig. 4 shows that non-PB-reinforced styrenics also display little change in LWIR. The peak at 965 cm^{-1}, framed in blue, is characteristic of vinylic C—H out-of-plane bending of PB whereas the 910 cm^{-1} is also associated with styrene (Saviello et al., 2014), as it can be seen on other shown materials. This first peak is thus the only one differentiating GPPS and SAN from HIPS and ABS in LWIR. However, it disappears at first measures, showing that PB oxidation occurs really fast, at least on surface. During ageing, a large bump rises from 1500 to 800 cm^{-1}, associated to C—O stretching. Whereas it culminates around 1200 cm^{-1} for artificially aged polymers, the bump top is rather around 1000 cm^{-1} for naturally aged samples. The first wavenumbers range corresponds to esters, whereas the second one is associated to ethers (Gardette et al., 1995) and could also correspond to alcohols. This difference is in correspondence to the stronger carbonyl peaks observed in accelerated ageing and discussed in **Part 3.4**, which focuses on this signal for all considered polymers. Alternatively, spectra on the full MIR range are available in supporting information. Interestingly enough, these bumps do not mask the relatively weak signals that were present from 1200 to 800 cm^{-1} but rise them up. Thus, all maxima observed after ageing were already present initially. The main characteristic peaks, for aromatic C—H deformations, at 750 + 695 cm^{-1} for HIPS and 760 + 700 for ABS (Signoret et al., 2019a), remain little affected.

The ATR defect, which gives a curved baseline, because of the dependence of infrared rays penetration depth to their wavenumber, is stronger with ageing as spacing between sample spectra is greater on the right-side of plots. It can be related to a deterioration of the surface. It is the main observed differences with aged SAN and ASA samples, more marked in artificial conditions. GPPS also displays this trend but a very subtle baseline rises from 1350 to 1200 cm^{-1}, especially in natural ageing, could be associated to esters formation, again in concordance with carbonyl formation whereas it is absent from SAN. This is consistent with the chemical resistance which acrylonitrile brings to the copolymer (Berko et al., 1992). That ABS however seems as impacted as HIPS can be explained by the higher PB content (Moore, 1973), which thus brings both more material to be oxidized and initiators toward SAN degradation.

3.1.2. Comparison to real waste samples

The polybutadiene characteristic peak at 965 cm^{-1} (blue frame) was found on only a few HIPS waste samples (Fig. 5) and a bit more frequently in ABS samples (Fig. 6), coherently with higher PB content of ABS. These samples were differentiated from GPPS or SAN by their ductile behavior, accompanied with strong whitening when deformed, whereas their counterparts are fragile and break without deformation or coloration. This peak absence from waste samples is coherent with its fast disappearance, which was observed during ageing tests. Oxidation marks, especially alcohols, carbonyls and ethers were observed on roughly two thirds of styrenics found within the studied waste stock, closer to results obtained with natural ageing than the artificial one. Aged references of Fig. 5 & Fig. 6 were chosen at 6 weeks of natural ageing (purple) and only 1 of accelerated ageing (red) as they already display spectra more altered than most of the ones encountered within the waste stock. Especially, some samples display spectra

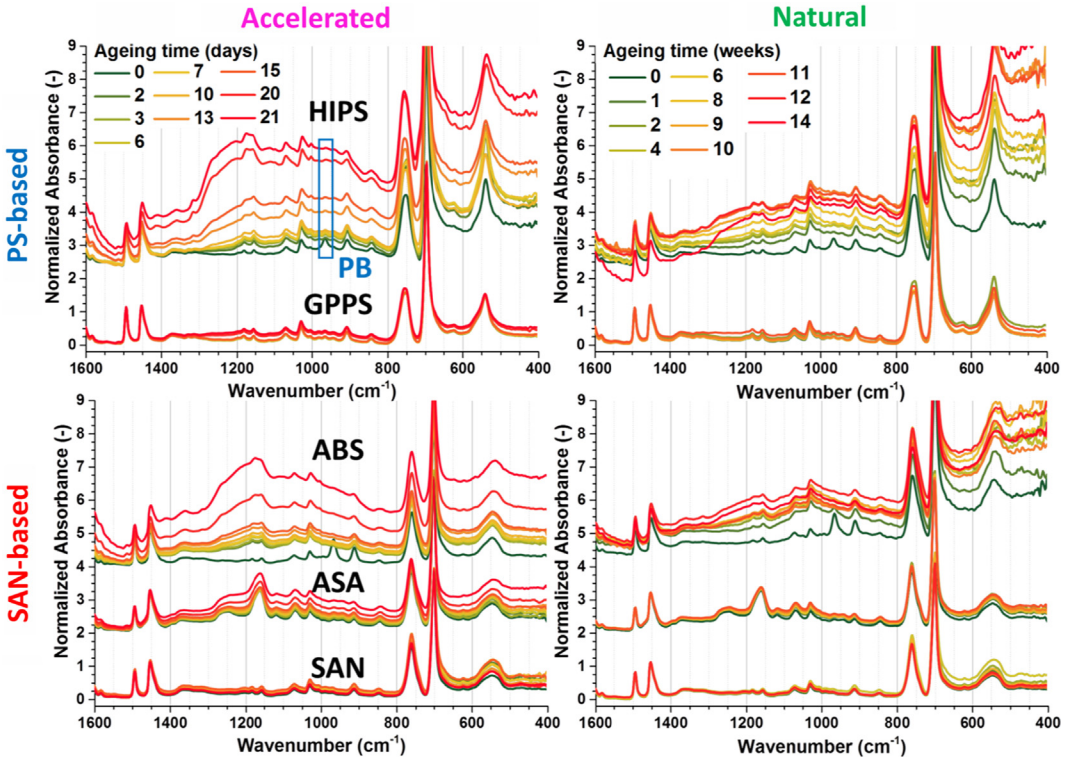

Fig. 4. FTIR-ATR spectra of styrenics aged in both accelerated and natural conditions – LWIR range – spectra normalized on the 1452 cm^{-1} peak height – blue frame for vinylic C—H bending of polybutadiene.

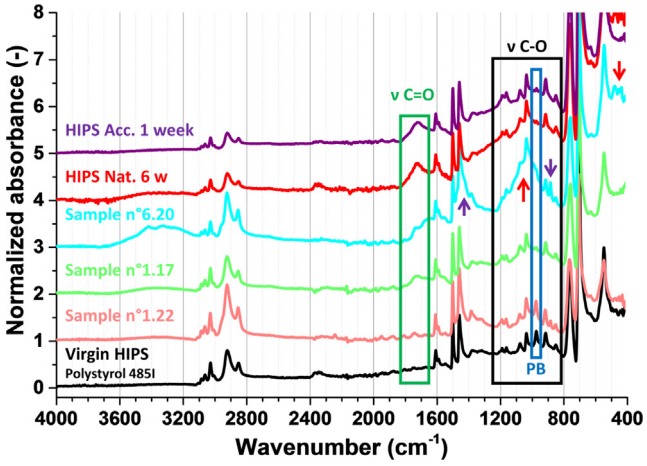

Fig. 5. MIR spectra comparison of 4 HIPS waste samples to virgin, naturally aged (6 weeks) and artificially aged (1 week) references spectra normalized on the 1452 cm^{-1} peak height – green frame for carbonyl peak, black frame for C—O peak, blue frame for 965 cm^{-1} PB peak – on sample 7.34: purple arrows for calcite marks (1405 + 873 cm^{-1}), red ones for possible talc marks (1010 + 670 cm^{-1}).

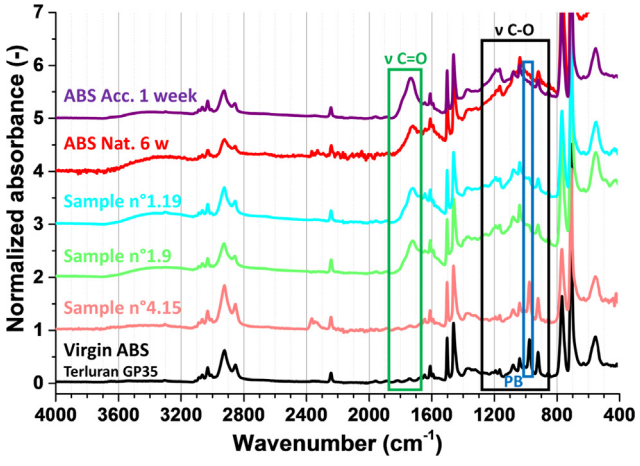

Fig. 6. MIR spectra comparison of 3 ABS waste samples to virgin, naturally aged (6 weeks) and artificially aged (1 week) references spectra normalized on the 1452 cm^{-1} peak height – 1 A.U. offsets for readability – green frame for carbonyl peak, black frame for C—O peak, blue frame for 965 cm^{-1} PB peak.

very close to the virgin reference, as sample n°1.22 on Fig. 5 and n °4.15 on Fig. 6 (both pale red).

In HIPS (Fig. 5), carbonyls were found more or less marked, often displaying a round bump as with sample n°1.17 (pale green). This sample also displays a weak O—H bump. Sample 6.20 (cyan) is misleading as it is among the rare styrenic samples loaded with mineral fillers. Calcite (purple arrows) is highlighted by the splayed shape of the 1450 cm^{-1} peak and a sharp peak at 873 cm^{-1} (Signoret et al., 2019b). Talc (red arrows) is shown through the peaks at the very limit of the spectrum, which are precisely at 465, 450 and 424 cm^{-1} and also participate to the C—O bump around 1010 cm^{-1}. The characteristic 670 cm^{-1} peak of talc (Signoret et al., 2019b) is however masked by the aromatic C—H peaks.

HIPS samples were found to be more frequently oxidized than ABS within the studied waste stock. However, ABS samples were found with stronger oxidation marks than HIPS when they showed some (samples 1.9 and 1.19 in pale green and cyan on Fig. 6). The O—H bump is especially visible and the carbonyl peak displays a different shape, more triangular with a shoulder. Again, ethers/alcohols C—O are favored compared to esters/acids as the bump is centered on 1000 cm^{-1} and O—H groups are related to alcohols rather than acids.

Samples within the waste stock were rapidly identified as styrenics thanks to the intense aromatic C—H deformation peaks at 750 + 695 cm^{-1} for HIPS and 760 + 700 cm^{-1} for ABS. It was also checked each time if they did not show foreign signals belonging to PC, PMMA, PPO (Signoret et al., 2019a). These samples did generally not show oxidation marks stronger than for 6 weeks of HIPS and 9 weeks of ABS natural ageing. This can be explained by their preferred indoor applications and the use of anti-UV additives, especially carbon black, as almost every considered styrenic sample was of dark color.

3.1.3. Conclusions on aged styrenics identification

MWIR identification seems not challenged as mainly alcohol functions were observed within the waste stock or after natural ageing. In accelerated ageing however, important carboxylic acids O—H signals were seen, masking the whole range, especially in HIPS. LWIR is more impacted as C—O signals appear on most of the range due to different chemical functions, esters, acids, ethers, conjugated or not. Natural ageing was found more coherent with the studied waste stock as they display bands centered on 1025 cm^{-1} instead of 1175 cm^{-1} for artificial ageing. Most important signals of LWIR, aromatic C—H, were still well defined but at the limit of spectral range. Other signals were still defined as well, but lifted up by C—O stretching which, in some ways, distort the baseline in LWIR. This means that automatized identification is still possible in MWIR despite ageing if a tolerance is given on O—H signals, which is also affected by atmospheric humidity, possibly very variable in industrial conditions. In LWIR, the problem is closer to a baseline distortion and adequate algorithms could be used to overcome this issue. Sadly, this could surely affect negatively signal-to-noise ratio and renders important signals hard to detect.

Discrepancies between natural and accelerated ageing in both MWIR and LWIR indicate that whereas artificial ageing leads to creation of numerous carbonyl based species, especially esters and acids, natural ageing is more confined to hydroxyls and ethers formation, hinting for relatively less chain scissions. This could be linked to different mechanism but could be more probably linked to a way more advanced degradation state, coherently to way more altered spectra. As ageing advances, predominant species are different depending to the different kinetics into play.

Even if most characteristic signals are shown to be preserved, both O—H and C—O apparition must be well taken into account not to disrupt classification. Indeed, matches with databanks identified most of oxidized HIPS samples as a copolymer of styrene and vinylic alcohol, which is not credible for such commercial applications. Also, as oxidation marks are similar between polymers, they can bring confusion into algorithms. It could be advisable to use laboratory aged samples, and laboratory formulated samples when building an identification algorithm. Thus, tolerances toward oxidation and fillers could be rightly developed, without other bias which could come from uncontrolled real waste samples. Finally, even if stabilized, one can only recommend protecting End-of-Life plastics from weathering before their valorization to avoid too important spectral alterations.

3.2. Polyolefins: PE & PP

3.2.1. Ageing of pristine references

Artificially aged PP shows yellowing and cracks, as Fig. 7 tries to relate. Even harder to show through a picture, artificially aged PE and naturally aged PP also developed cracks, in a lighter measure. Naturally aged PE does not display visual significant changes. Yellowing of artificially aged PP means that conjugated species appeared, probably derived from oxidized species produced during chain scissions mechanisms(Vaillant et al., 1994). However, the

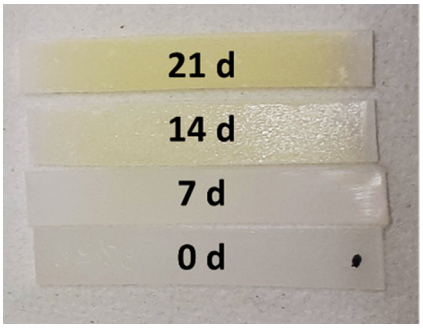

Fig. 7. Picture of artificially weathered PP samples.

lack of unsaturated groups as phenyls in styrenics hampers rapid conjugation, and thus strong discoloration (Signoret et al., n.d).

Fig. 8 shows that polyolefins are moderately impacted in MWIR, especially PE. As with styrenics, two bumps can be seen on artificially aged PP, the left-sided one corresponding to alcohols being way more pronounced. C—H stretching of PP from 2950 to 2835 cm^{-1} seems to decrease in both ageing modes. The most plausible explanation is the influence of the ATR defect (confirmed on Fig. 9) as normalization was done with the 1452 cm^{-1} peak, which is associated to CH_2 deformation, relatively "far" from the range considered here. This hints that the relatively important observed alcohol bump is even stronger than it appears. Subtle alcohol O—H apparition also occurs within artificially aged PE whereas PE in natural ageing displays no visible changes. Identification should not be impacted if PP hydroxyls are considered separately.

Fig. 9 shows that polyolefins are more impacted in LWIR, but mostly in artificial conditions, with for main feature the apparition of C—O bonds. After accelerating ageing, both PE and PP display C—O stretching bumps culminating just below at respectively 1170 and 1167 cm^{-1}, corresponding to esters. The 1167 cm^{-1} top in PP corresponds to a peak that was already there and got lift up, as seen with styrenics previously. In both polyolefins, a shoulder is clearly visible at 1240 cm^{-1}, hinting for differences in esters conjugation, concordantly with multimodal carbonyl peaks described in **Part 3.4**. In natural ageing, C—O stretching apparitions are way more discreet, confined to little bumps at 1035 cm^{-1} for PE and 1040 for PP, associated to ethers or alcohols, and not esters. Relatively weak intensities of corresponding carbonyls corroborate these results. This hints that oxidation in natural ageing occurs without much chain scissions in these conditions and durations as this phenomenon is often associated to carbonyls apparition (Chabira et al., 2012; Gardette et al., 2013). Baseline distortion due to ATR is also important, as seen with styrenics. It is also more distinct in accelerated ageing especially for PP, fittingly with its degraded surface featuring cracks. Minor peaks can also be observed, framed in blue on artificially aged samples spectra, corresponding to vinylic C—H deformation. Only one is clearly visible at 910 cm^{-1} for PE but two at 940 and 760 for PP. Their presence matches with the C=C stretching observed at 1640 cm^{-1} shown in **Part 3.4** and supporting information, especially as they are more visible in PP since it is more subject to Norrish II reactions which generate them. Indeed, chain scission is the main mechanism observed in PP degradation (Luzuriaga et al., 2006). The dissimilarity between PE and PP vinylic C—H peaks in wavenumbers can be explained by the vinyl substitution differences originating from the chemical nature of the polymers building blocks.

Fig. 10 displays magnification of respective crystallinity markers with numerical offsets for readability. Duality of certain signals reflects crystallinity: 1470 + 1460 cm^{-1} for CH_2 deformation and 730 + 720 cm^{-1} for $(CH_2)_{n>2}$ in the case of PE (Hagemann et al.,

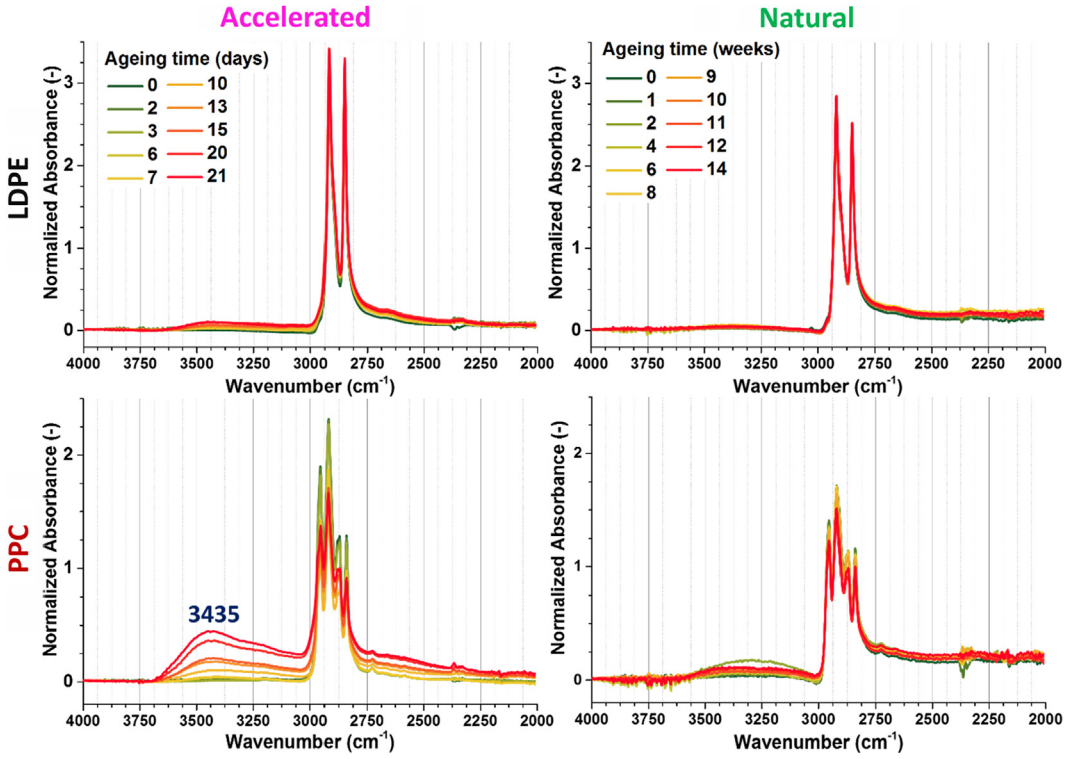

Fig. 8. FTIR-ATR spectra of polyolefins aged in both accelerated and natural conditions – MWIR range – spectra normalized on the 1452 cm^{-1} peak height.

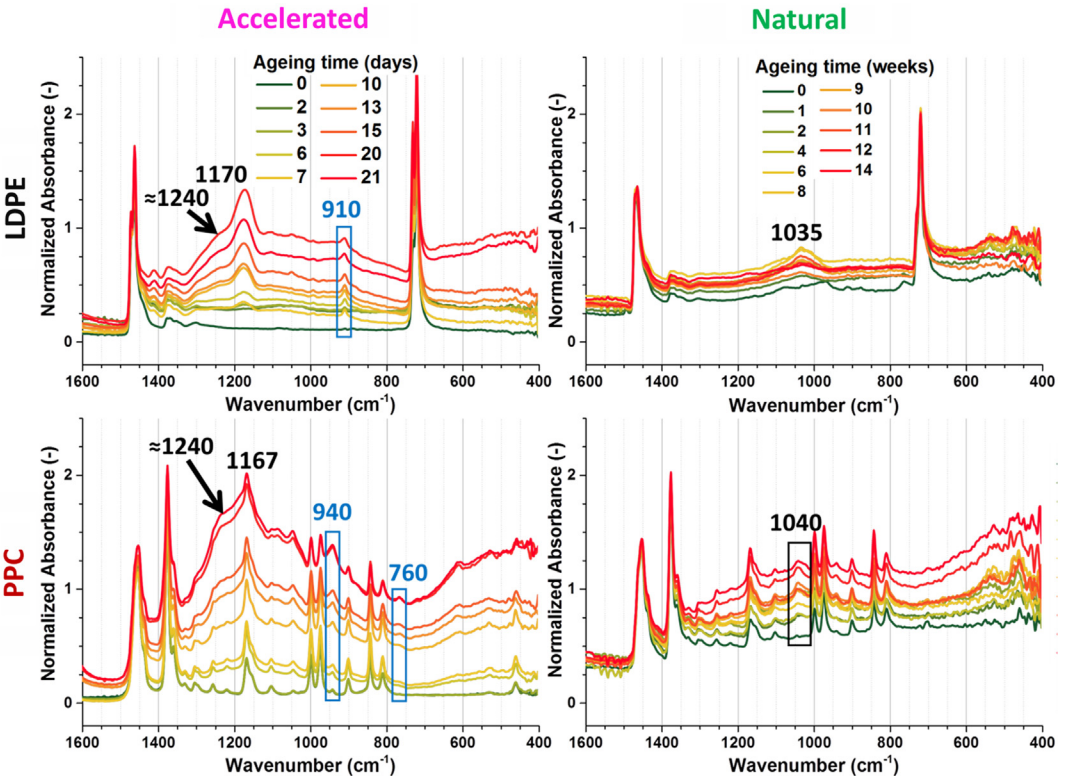

Fig. 9. FTIR-ATR spectra of polyolefins aged in both accelerated and natural conditions – LWIR range – spectra normalized on the 1452 cm^{-1} peak height – black frames and annotations for C—O (esters, ethers or alcohols) – blue frames for vinylic peaks.

1989; Noda et al., 2007) and 1375 + 1360 for CH_3 deformation of PP (Luongo, 1960). Duality for PP is more subtle as the "second peak" is only a shoulder at about 1435 cm^{-1} for a main peak around 1455 cm^{-1}. LDPE displays crystallization with accelerated ageing as duality is more and more marked, with the rise of 1470 and 730 cm^{-1} peaks, characteristic of crystalline phases (Hagemann et al., 1989), formed from chain scission. It is not the case with naturally weathered PE, except perhaps for the last measure, indicat-

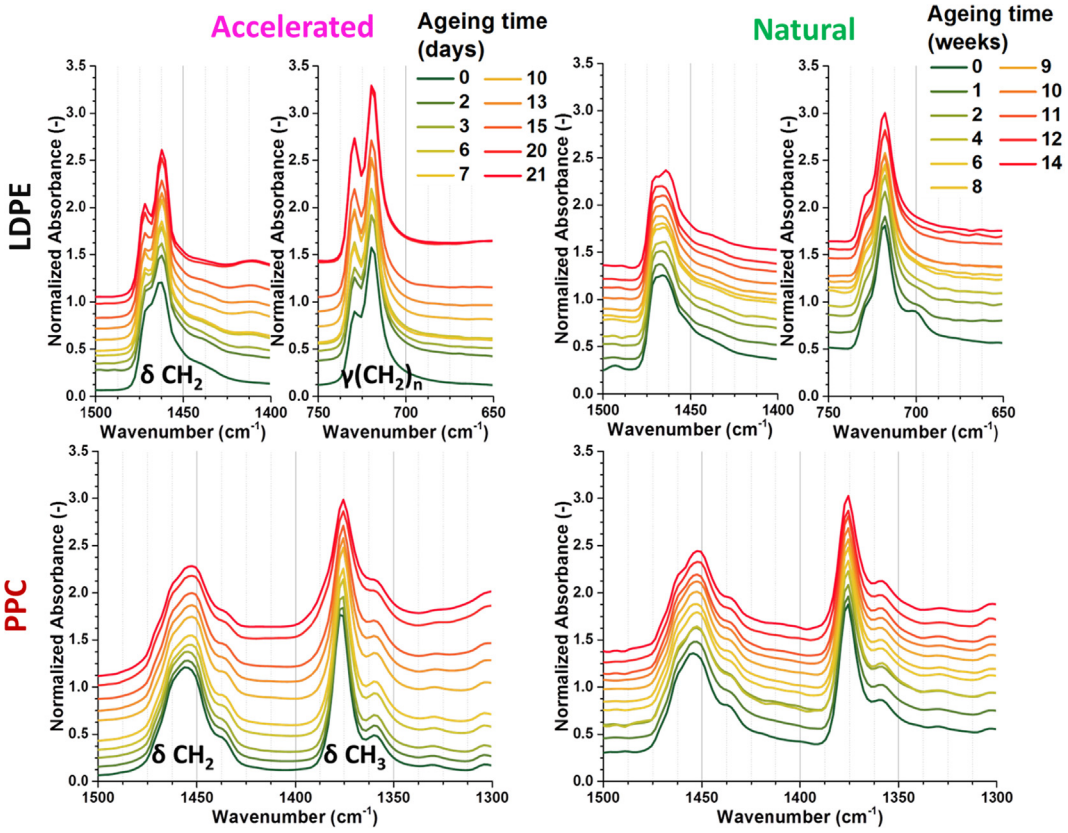

Fig. 10. FTIR-ATR spectra of polyolefins aged in both accelerated and natural conditions – magnification on crystallinity markers (1500–1400 & 750–650 cm^{-1} for PE, 1500–1300 cm^{-1} for PP) – spectra normalized on the 1452 cm^{-1} peak height – 0.1 A.U. offsets for readability.

ing that chain scission is less important, as absence of oxidized species corroborates. Artificially aged PP shoulder is more and more important, progressively convoluting with the main peak more and more but features are less clear than with PE. Naturally aged PP does not display significant changes.

3.2.2. Comparison to real waste samples

Fig. 11 shows comparison of PE real waste samples compared to unaged, 2 weeks artificially aged and 11 weeks naturally aged samples, in order to be as close as possible to the most extreme encountered real cases. Real samples display oxidation marks closer to the naturally aged reference, as the two subtle bumps in sample 2.8 (light green) or the very similar spectrum of sample n °1.30. Sample n°1.26 shows a carbonyl peak, close to what was observed in accelerated ageing for the first days. Though, the peak around 1000 cm^{-1} is surely mainly due to talc presence which is corroborated by the 670 cm^{-1} and 465–400 cm^{-1} peaks (red arrows). Crystallinity features are rash to consider as they are also subject to the sample nature (e.g. LDPE/HDPE), molecular mass and thermal history.

Fig. 12 compares PP real waste samples to references aged similarly to PE. As with PE, numerous peaks due to fillers could be mis-

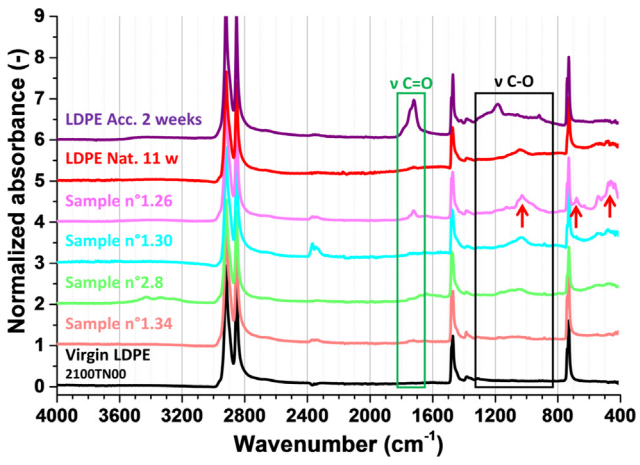

Fig. 11. MIR spectra comparison of 4 PE waste samples to virgin, naturally aged (11 weeks) and artificially aged (2 weeks) LDPE references spectra normalized on the 1466 cm^{-1} peak height – 1 A.U. offsets for readability – green frame for carbonyl peak, black frame for C—O peak - red arrows on 1.26 for talc marks.

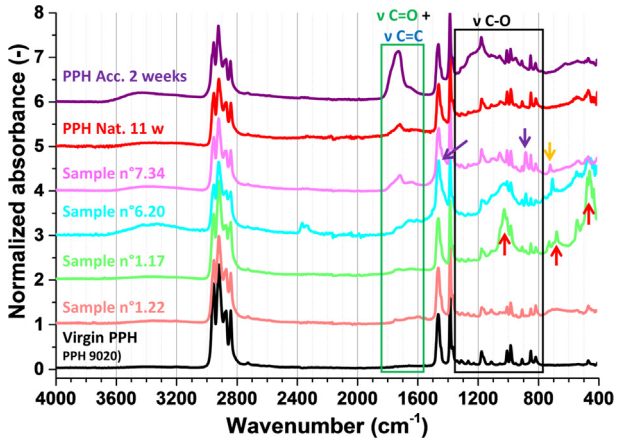

Fig. 12. MIR spectra comparison of 4 PP waste samples to virgin, naturally aged (11 weeks) and artificially aged (2 weeks) PPH references spectra normalized on the 1452 cm^{-1} peak height – 1 A.U. offsets for readability - green frame for carbonyl peak, black frame for C—O peak– purple arrows for calcite marks, red ones for possible talc marks, orange one for 720 cm^{-1} peak of $(CH_2)_n$.

taken and/or convolute with oxidation marks. Red arrows indicate talc in samples n°1.17 (light green) and 6.20 (cyan). Purple ones indicate calcite in samples n°6.20 and 7.34 (light pink). This last spectrum also displays a peak at 730 cm^{-1} (orange arrow) which characterize ethylene units. Thus, this sample can be categorized as polypropylene copolymer.

3.2.3. Conclusions on aged polyolefins identification

Differences in ageing marks were highlighted between accelerated ageing and natural ageing for PE in this case. Here, oxidation occurred without much chain scission in natural conditions with formation of alcohols or ethers whereas artificially aged PE formed esters, acids and other carbonyl-based species, related to chain scissions mechanisms, probably indicating that it reached a more advanced degradation state.

With artificial weathering, observed evolutions of both PE and PP could disrupt identification in MWIR if variations due to hydroxyls are not taken into account. Conversely, natural ageing lead to way milder modifications, closer to what was encountered within the studied waste stock.

For LWIR, C—O peaks appear in PE but do not disturb other peaks. In PP however, the whole baseline is altered, and characteristic signals lift up. In natural ageing, changes are way more moderate, with principally the ATR defect amplifying and alcohol formation in PP. Real waste samples were more impacted by bad surface aspect, which hindered good acquisition. However, the effects of bad surface aspect on quality can difficultly comparable between HSI and FTIR-ATR as one measure is remote and the second relies on crystal-sample contact quality. Peaks which could be attributed to oxidation at first glance were actually often due to high filler loadings. Identification is still possible, but new signals must be taken into account for what they are, especially in automatized classification.

3.3. Polycarbonate

In both artificial and natural conditions, polycarbonate plates were subject to an important yellowing in the first tens of microns as Fig. 13 **a)** presents on naturally aged samples. This yellowing is well explained in the literature by the "Photo-Fries" mechanism (Rivaton, 1995). However, no important modifications are exhibited on corresponding FTIR-ATR spectra (Fig. 13 **b)**) and those of the two real waste samples. One slight difference could be found in relative intensities. Whereas natural ageing just slightly increases the ATR curvature with ageing as surface aspect degrades, artificial ageing also leads to C═O and C—O elongation signals decreases. This can be attributed to the structural modification due to the Photo-Fries mechanism which permutes carbonate function to ketones and alcohols (Rivaton, 1995). In previous works (Signoret et al., n.d), we could notice that yellowing was visually observed without spectral modification for GPPS and SAN. Also, recycling photodegraded styrenics showed that color is more sensitive to these modifications than infrared spectroscopy. Nevertheless, other studies (Collin et al., 2012; Moustaghfir et al., 2005) lead to strong spectral modifications of photodegraded PC, hinting that ageing was not conducted long enough in the present case.

Identification of PC does not seem to be perturbed by ageing in the current frame as spectra are almost unaltered. Within the studied waste stock, only two PC samples were available, also exhibiting spectra close to virgin references. Stronger ageing conditions and more numerous real waste samples are advisable for more confident conclusions. However, mild spectral modifications are to be related to the described ageing mechanisms which does not create very different chemical bonds from those already existing (Rivaton, 1995).

3.4. Carbonyl peak in polymers: Intrinsic or ageing-dependent

3.4.1. Ageing of pristine references

Even if currently out of range for MWIR and LWIR, the carbonyl peak is very specific and rich in information. It is thus a useful tool for rapid assessment of plastic samples at laboratory scale and hopefully someday in industrial conditions. Fig. 14 gathers all carbonyl peaks of the present study. "Intrinsic" carbonyl peaks, as with ASA or PC are rather sharp, no more than a hundred cm^{-1}

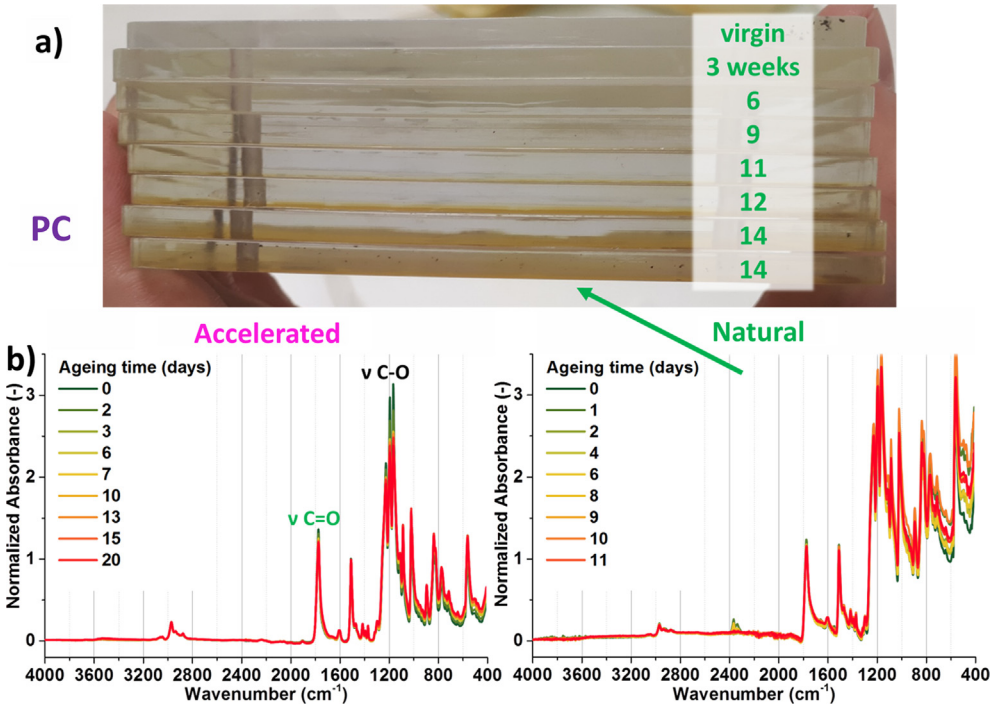

Fig. 13. a) Picture of naturally aged polycarbonate plates – exposed faces toward bottom b) FTIR-ATR spectra of PC aged in both accelerated and natural conditions – MIR range – spectra normalized on the 1502 cm^{-1} peak height.

wide at the base and less than 25 cm^{-1} wide near the top. However, carbonyl peaks due to ageing are larger, up to 200 cm^{-1} large for HIPS or ABS, with "rounder" features. The convolution of several peaks is quite visible since several shoulders are seen, especially with artificially aged LDPE and ABS. By their different chemical natures, the polymers studied here foster different carbonyl species, resulting in different peaks and shoulders positions.

Virgin ABS displays a peak at 1640 cm^{-1}, corresponding to vinylic C=C stretching of PB (Saviello et al., 2014). Thus it is absent from GPPS, SAN or ASA. As HIPS contains less PB (in concordance with 965 cm^{-1} relative intensities of Fig. 4), this peak is not seen here. Interestingly enough, whereas the 965 cm^{-1} peak, associated to trans vinylic C—H bending, rapidly disappears with ageing, this peak is visible for large ageing periods. This is coherent with the mechanism described by Gardette et al.(Gardette et al., 1995), where the carbon in alpha position reacts whereas the double bond is preserved.

HIPS and ABS conduct to very similar carbonyl bands. Because of their chemical likeness, they share an important part of their oxidation reactions paths (Mailhot and Gardette, 1994). In accelerated ageing, the top is observed at 1710 cm^{-1} for the first one and 1713 cm^{-1} for the second, which is more marked as this value stands out more distinctly. These wavenumbers are associated to carboxylic acids (Gardette et al., 1995; Saviello et al., 2014), in accordance with large O—H bands centered on 3000 cm^{-1} on Fig. 3 and C—O bands around 1200 on Fig. 4.

They also share a shoulder (indicated by arrows on Fig. 14) at roughly 1780 cm^{-1} that Piton et Rivaton (Piton and Rivaton, 1997) assigned to the convolution of α,β-unsaturated anhydride, perester and γ-lactones. The impressive base width of the peak is due to very large number of formed species finely described by Gardette al. (Gardette et al., 1995), vibrating from 1540 cm^{-1} for 1,3-diphenyl-1,3-propanedione to 1785 cm^{-1} for benzoic anhydride. It is more plausible that the difference of peak top wavenumbers is due to the same conjugation and inductive effects that differentiate their aromatic C—H deformations (695 + 750 $cm^{-1}$for HIPS, 700 + 760 cm^{-1} for ABS), than to differences in formed oxidized species. Especially, the wavenumbers shifts are of the same order of magnitude. That these spectral differences are observed macroscopically without peak duplication indicates that acrylonitrile units are homogenously scattered along the chains. Natural ageing lead them to similar features, in a less advanced state. On last measures (2 weeks of accelerated ageing & 12 weeks of natural ageing), GPPS develops a weak signal with a similar width in spite of its height. Concordantly with Fig. 3 & Fig. 4, SAN remains spectrally unaltered even if a slight yellowing is observed (Signoret et al., n.d). As ASA initially has a carbonyl peak, it displays a widening of this band in both ageing types.

The artificially aged LDPE carbonyl peak displays a very characteristic stairs-like shape that Gardette et al. (Gardette et al., 2013) described as the convolution of carboxylic acid, ketone, ester (shoulder at ≈1735 cm^{-1}), lactone (shoulder at ≈1785 cm^{-1})… among others. The visually sharper shape of the peak in comparison to styrenics can be explained by the absence of the 1700–1600 cm^{-1} part, which was mainly associated to species conjugated with phenyl groups present in their chemical structure. However, a small bump can be observed on the last measurements of accelerated ageing, about 1640 cm^{-1}, corresponding to C=C stretching, produced by Norrish II photochemical reactions of ketones (Gardette et al., 2013). In the present case, natural ageing only leads to a little a bump at 1713 cm^{-1}, only on very last measurements. It is coherent with the lack of new signals shown on Fig. 8 & Fig. 9 but also with Fig. 10 where crystallinity increased progressively with natural ageing but was noticeable on the last curve for artificial conditions. Oxidized species mentioned above being often linked to chain scissions, their presence is to be correlated with crystallinity improvements. PPH displays similar results but with more intense signals, hinting for a higher sensitivity to chain scission than LDPE. Also, the 1713 cm^{-1} peak is relatively less pronounced in comparison to the 1735, 1770 and 1640 cm^{-1} shoulders, giving a rounder shape to the general signal. Natural ageing produced a triangular shape, which can be retrieved on first measurements of accelerated ageing (especially at 10 days).

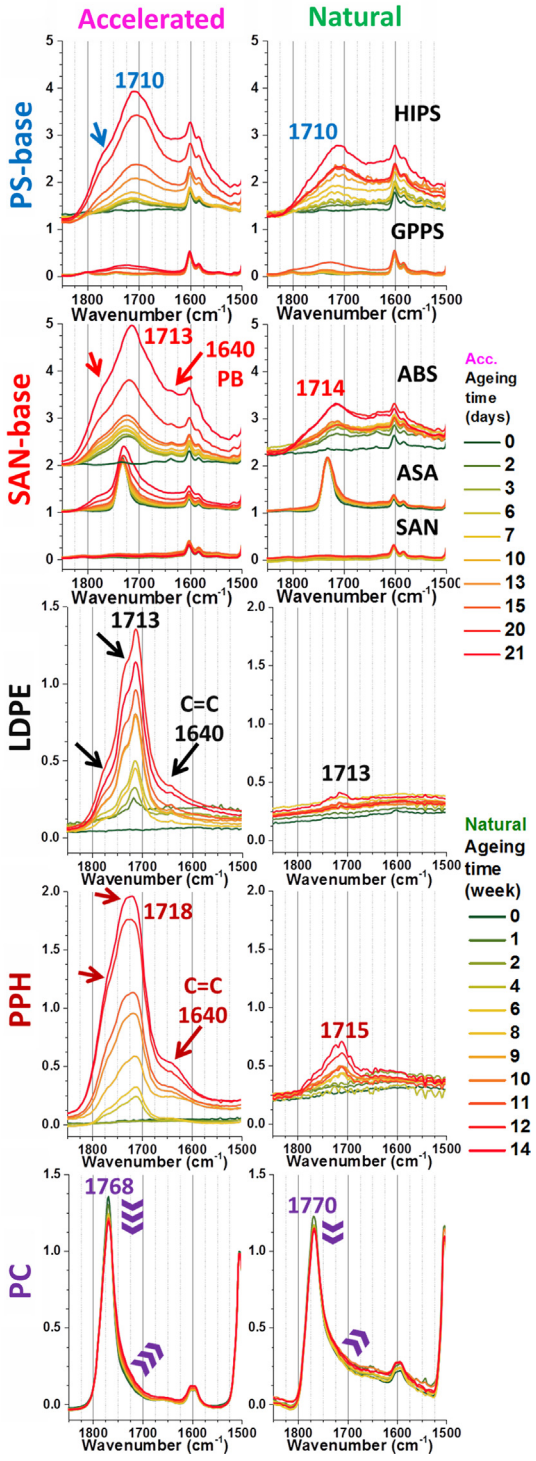

Fig. 14. Carbonyl peaks of aged polymer references –absorbance normalized on the 1452 cm^{-1} peak heights, except for PC with the 1502 one – baselines adjusted at the left limit of the carbonyl peaks – arrows indicate peaks shoulders & chevrons indicate evolution directions.

As discussed above, PC did not spectrally evolve much during the present study despite visual changes. However, a closer look on Fig. 14 reveals that the peak top at 1768 cm^{-1} decreased in intensity whereas its right-handed base slightly rose around 1720. This subtle change is coherent with the observed yellowing and its justification by the Photo-Fries mechanism where carbonate functions (1770 cm^{-1}) are transformed into different ketones and other species absorbing at lower wavelengths (Rivaton, 1995). Natural ageing leads to similar but milder results than accelerated ageing.

3.4.2. Intrinsically carbonyl containing polymers

Fig. 15 gathers references of several commercial carbonyl containing polymers, most of them encountered within the waste stock. Interestingly enough, wavenumbers are spaced by more than 10 cm^{-1} (except for ASA/EVA): PA at 1635, PET at 1713, PMMA at 1722, ASA at 1732, EVA at 1736, PLA at 1747 and ABSPC/PC at 1768. These differences can be easily explained by the very different chemical environments of these carbonyls. A table of polymer carbonyl peaks with corresponding formulas is available in supporting information paragraph E. PU can display two C═O signals, one at 1700–1710 cm^{-1} for H-bonded urethane and one at 1730–1735 cm^{-1} for free urethane (Sonnenschein, 2014). The PU family is very wide, including every form of polymers: thermoplastics, thermosets, elastomers and foams, of various chemical natures. These materials often display a relatively complex chemical structure compared to other polymers (Chattopadhyay and Webster, 2009) and representing the whole family through a few samples is complicated without further research.

All of mentioned polymers do not just contain carbonyls by themselves but in the form of ester, amide, carbamide and carbonate functions, more or less conjugated. Thus, polyamides also display signals associated to N-H deformation around 1635 cm^{-1} at similar height as the carbonyl peak. And the other display C—O stretching in the 1300–1000 cm^{-1} range (within LWIR). These patterns are very distinctive for each of them, as it can be seen on Fig. 15 (black frame) or in the *supporting information* complete LWIR chart. PET (and PBT in *supporting information*) has two strong spaced signals at ≈1240and ≈1100 cm^{-1}. Most PUs have similar but wider and richer patterns similarly to the one presented here. PLA (more visible in *supporting information*) and PMMA have couples of peak groups with a gap between them. The first parts are respectively from 1270 to 1180 cm^{-1} and from 1280 to 1200 cm^{-1} and the second parts are respectively from 1130 cm^{-1} to 1000 cm^{-1} and from 1200 to 1060 cm^{-1} with maxima respectively at 1080 and 1142 cm^{-1}. PC has three close peaks with growing heights at 1219, 1187 and 1158 cm^{-1}. ASA and EVA are relatively free of signals, mainly single peaks respectively at 1161 and 1236 cm^{-1}, explicable as C—O bonds are part of minority components (28 w% vinyl acetate in the presented reference). Outside of this range, PET and PBT also feature very strong signals at 720 cm^{-1} for their chaining CH_2 out-of-plane deformation, which is relatively stronger in the second one because of their respective chemistries. PA and PU also have a strong peak at 1540 cm^{-1} (out of LWIR) associated to N-H bending.

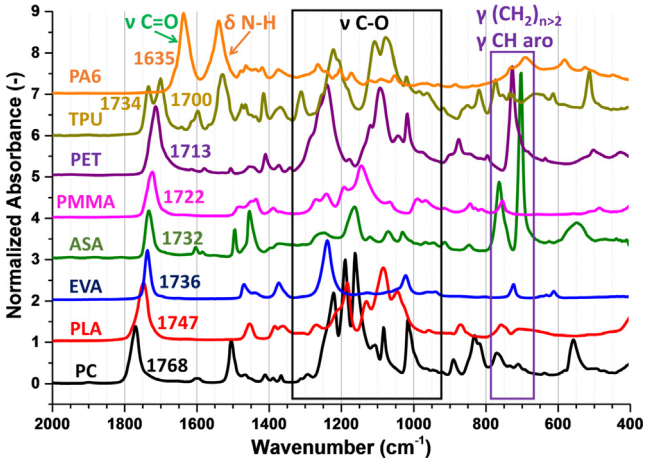

Fig. 15. Intrinsic carbonyl peaks of virgin polymer references: PA6 (Technyl C206), TPU (Irogran A90P 5055), PET (Multiflex SIE s 7007 SPA1), PMMA (Altuglas V825T), PLA (PLI 004) & PC (Makrolon 2805) - from 2000 to 400 cm^{-1}.

3.4.3. Conclusions on the carbonyl peak as an identification tool

These considerations helped to rapidly identify numerous samples within the waste stock by assessing the carbonyl wavenumber then visually double-checking with C—O patterns. As discussed on laboratory samples, aged samples of polyolefins or styrenics displayed carbonyls with far weaker intensities and larger widths than those of polymers containing intrinsically carbonyls as they correspond to a multitude of species, more or less conjugated, that appear rather sparsely along the chains whereas "intrinsic" carbonyls appear at each monomer unit. Also, their top wavenumbers are confined between 1710 and 1715 cm^{-1} for styrenics and 1710–1720 cm^{-1} for polyolefins whereas "intrinsic" carbonyls range from 1635 to 1770 for considered polymers. Carbonyls issued from ageing can also be the visible result of convolutions of several peaks, which is rarely the case with "intrinsic" carbonyls, with the exception of the dual peak of some PU. Interestingly enough, "intrinsic" carbonyls are sufficiently different in wavenumbers to enable fast identification, even at degraded resolution. Also, the very specific but also very rich patterns of C—O stretching in LWIR make laboratory identification easier and more confident. This could however be disadvantaging in industrial applications as they mean more data management. Also, decreased resolutions can result in amorphous signal clusters difficult to analyze.

4. Conclusions

As a surface phenomenon, polymer ageing is a concern for various plastic separation processes, especially optical ones. This study's primary objective was to evaluate its possible impacts on MIR-HSI, a technology in development for the sorting of dark colored End-of-Life plastics to design advanced recycling facilities. As a secondary objective, this can help difficult laboratory identification of degraded polymers through FTIR. In this purpose, styrenics, polyolefins and polycarbonate pristine references were photodegraded in natural and artificial conditions and their spectra assessed.

Styrenics ageing was concerning in MWIR (2–5 μm or 5000–2000 cm^{-1}) for artificially aged HIPS, as new signals masked the whole range. In natural conditions and on real waste samples, spectra were however still easily identifiable. Polyolefin identification in MWIR is not compromised if the new features are taken into account. More important features were observed in LWIR (7.4–14.0 μm or 1350–700 cm^{-1}) for styrenics and polyolefins, especially because of C—O formation on the whole range, more or less expressed by baseline deformation with polymer characteristic peaks preserved. Many features, which could be granted on ageing within the waste stock, were in fact to be attributed to fillers as they display similar large features in the same ranges. Most of waste samples displayed ageing marks milder than those of laboratory aged references in accordance with the use of stabilization systems, important dark coloration and indoor uses of studied stocks, especially for styrenics. Moreover, natural ageing and accel-

erated ageing did not lead to exactly the same signals for most references, probably indicating different degrees of degradation. The carbonyl peak, off-limits for current commercial hyperspectral cameras, enables rapid identification of several polymers as PA, PMMA, PET or PC. Carbonyls due to ageing are often larger and less intense enabling rapid differentiation from "intrinsic" carbonyls. This could be of great help for laboratory analysis and could lead to great industrial sorting improvements if HSI technology reach this range.

It could be interesting to segregate too severely photodegraded materials during mechanical recycling as they can impair mechanical properties. However, oxidation thresholds are to be defined, probably differently from a polymer to another, and from a specific application to another. Finally, this present study assessed only ageing of unformulated samples and direct comparison to real waste samples. Evaluation of other polymers ageing and other ageing modes (thermooxidation, natural ageing in other climates, photooxidation in finer conditions...) could greatly enrich these considerations. Spectral alteration was mainly studied here but surface aspect deterioration could be more concerning toward industrial identification. Also, complementary studies on the interaction with photoprotection systems from the simple use of carbon black to HALs systems, use of fillers or possibly prodegradant additives as flame retardants, both on their possible impact ageing and the combination of these effects on spectral alteration toward identification could permit a refining in automatized sorting technologies and thus more valuable recyclates.

Funding

This work was supported by BPI France via the FUI 20 (Fonds unique interministériel) grant and Suez internship funding.

Declaration of Competing Interest

The authors declare that they have no known competing financial interests or personal relationships that could have appeared to influence the work reported in this paper.

Acknowledgements

The authors would like to thank Benjamin Gallard, Robert Lorquet, Romain Ravel and Alain Diaz for technical support, respectively for polymer processing, spectroscopy, accelerated ageing and handiwork. Pierre-Alain Ayral, Brahim Mazian and Jean-Francois Didon-Lescotthe from the Saint-Christol-lez-Alès weather station for their support in meteorological monitoring. Solange Madec, Danièle Larroze, Lydie Baroni and Sylvie Beuhorry are acknowledged for administrative support. Suez and Pellenc ST are gratefully acknowledged for partnership in this work.

Appendix A. Supplementary material

Supplementary data to this article can be found online at https://doi.org/10.1016/j.wasman.2020.04.043.

References

Akhshik, M., Panthapulakkal, S., Tjong, J., Sain, M., 2019. The effect of lightweighting on greenhouse gas emissions and life cycle energy for automotive composite parts. Clean Technol. Environ. Policy 21, 625–636. https://doi.org/10.1007/s10098-018-01662-0.

Alassali, A., Fiore, S., Kuchta, K., 2018. Assessment of plastic waste materials degradation through near infrared spectroscopy. Waste Manag. 82, 71–81. https://doi.org/10.1016/j.wasman.2018.10.010.

Allizé-Plasturgie, n.d. Allizé-Plasturgie : a professional organisation at the service of plastics and composites | Allizé-Plasturgie [WWW Document]. URL https://www.allize-plasturgie.org/allize-plasturgie-professional-organisation-service-plastics-and-composites (accessed 12.3.18).

Andrady, A.L., 2017. The plastic in microplastics: A review. Mar. Pollut. Bull. 119, 12–22. https://doi.org/10.1016/j.marpolbul.2017.01.082.

Bae, J.-S., Oh, S.-K., Pedrycz, W., Fu, Z., 2019. Design of fuzzy radial basis function neural network classifier based on information data preprocessing for recycling black plastic wastes: comparative studies of ATR FT-IR and Raman spectroscopy. Appl. Intell. 49, 929–949. https://doi.org/10.1007/s10489-018-1300-5.

Beigbeder, J., Perrin, D., Mascaro, J.-F., Lopez-Cuesta, J.-M., 2013. Study of the physico-chemical properties of recycled polymers from waste electrical and electronic equipment (WEEE) sorted by high resolution near infrared devices. Resour. Conserv. Recycl. 78, 105–114. https://doi.org/10.1016/j.resconrec.2013.07.006.

Berko, H., Hill, D.J.T., O'Donnell, J.H., Pomery, P.J., 1992. Photo-oxidative degradation of copolymers of acrylonitrile with styrene, α-methylstyrene and p-methylstyrene. Polym. Degrad. Stab. 37, 85–90. https://doi.org/10.1016/0141-3910(92)90096-N.

Boldizar, A., Möller, K., 2003. Degradation of ABS during repeated processing and accelerated ageing. Polym. Degrad. Stab. 81, 359–366. https://doi.org/10.1016/S0141-3910(03)00107-1.

Brennecke, D., Duarte, B., Paiva, F., Caçador, I., Canning-Clode, J., 2016. Microplastics as vector for heavy metal contamination from the marine environment. Estuar. Coast. Shelf Sci. 178, 189–195. https://doi.org/10.1016/j.ecss.2015.12.003.

Celina, M.C., 2013. Review of polymer oxidation and its relationship with materials performance and lifetime prediction. Polym. Degrad. Stab. 98, 2419–2429. https://doi.org/10.1016/j.polymdegradstab.2013.06.024.

Chabira, S.F., Sebaa, M., G'sell, C., 2012. Oxidation and crosslinking processes during thermal aging of low-density polyethylene films. J. Appl. Polym. Sci. 124, 5200–5208. https://doi.org/10.1002/app.34080.

Chattopadhyay, D.K., Webster, D.C., 2009. Thermal stability and flame retardancy of polyurethanes. Prog. Polym. Sci. 34, 1068–1133. https://doi.org/10.1016/j.progpolymsci.2009.06.002.

Collin, S., Bussière, P.-O.O., Thérias, S., Lambert, J.-M.M., Perdereau, J., Gardette, J.-L. L., 2012. Physicochemical and mechanical impacts of photo-ageing on bisphenol a polycarbonate. Polym. Degrad. Stab. 97, 2284–2293. https://doi.org/10.1016/j.polymdegradstab.2012.07.036.

Du, Y., Gao, J., Yang, J., Liu, X., 2012. Dynamic rheological behavior and mechanical properties and of PVC/ASA blends. J. Polym. Res. 19, 9993. https://doi.org/10.1007/s10965-012-9993-3.

Gall, S.C., Thompson, R.C., 2015. The impact of debris on marine life. Mar. Pollut. Bull. 92, 170–179. https://doi.org/10.1016/j.marpolbul.2014.12.041.

Gallo, F., Fossi, C., Weber, R., Santillo, D., Sousa, J., Ingram, I., Nadal, A., Romano, D., 2018. Marine litter plastics and microplastics and their toxic chemicals components: the need for urgent preventive measures. Environ. Sci. Eur. 30, 13. https://doi.org/10.1186/s12302-018-0139-z.

Gardette, J.-L., Mailhot, B., Lemaire, J., 1995. Photooxidation mechanisms of styrenic polymers. Polym. Degrad. Stab. 48, 457–470. https://doi.org/10.1016/0141-3910(95)00113-Z.

Gardette, M., Perthue, A., Gardette, J.-L., Janecska, T., Földes, E., Pukánszky, B., Therias, S., 2013. Photo- and thermal-oxidation of polyethylene: Comparison of mechanisms and influence of unsaturation content. Polym. Degrad. Stab. 98, 2383–2390. https://doi.org/10.1016/j.polymdegradstab.2013.07.017.

Grégoire, S., Boudinet, M., Pelascini, F., Surma, F., Detalle, V., Holl, Y., 2011. Laser-induced breakdown spectroscopy for polymer identification. Anal. Bioanal. Chem. 400, 3331–3340. https://doi.org/10.1007/s00216-011-4898-2.

Gundupalli, S.P., Hait, S., Thakur, A., 2017. A review on automated sorting of source-separated municipal solid waste for recycling. Waste Manag. 60, 56–74. https://doi.org/10.1016/j.wasman.2016.09.015.

Hagemann, H., Snyder, R.G., Peacock, A.J., Mandelkern, L., 1989. Quantitative infrared methods for the measurement of crystallinity and its temperature dependence: polyethylene. Macromolecules 22, 3600–3606. https://doi.org/10.1021/ma00199a017.

Jouan, X., Gardette, J.L., 1992. Photo-oxidation of ABS: Part 2—Origin of the photodiscoloration on irradiation at long wavelengths. Polym. Degrad. Stab. 36, 91–96. https://doi.org/10.1016/0141-3910(92)90054-9.

Kassouf, A., Maalouly, J., Rutledge, D.N., Chebib, H., Ducruet, V., 2014. Rapid discrimination of plastic packaging materials using MIR spectroscopy coupled with independent components analysis (ICA). Waste Manag. 34, 2131–2138. https://doi.org/10.1016/j.wasman.2014.06.015.

Kedzierski, M., D'Almeida, M., Magueresse, A., Le Grand, A., Duval, H., César, G., Sire, O., Bruzaud, S., Le Tilly, V., 2018. Threat of plastic ageing in marine environment. Adsorption/desorption of micropollutants. Mar. Pollut. Bull. 127, 684–694. https://doi.org/10.1016/j.marpolbul.2017.12.059.

Luongo, J.P., 1960. Infrared study of polypropylene. J. Appl. Polym. Sci. 3, 302–309. https://doi.org/10.1002/app.1960.070030907.

Luzuriaga, S., Kovářová, J., Fortelný, I., 2006. Degradation of pre-aged polymers exposed to simulated recycling: Properties and thermal stability. Polym. Degrad. Stab. 91, 1226–1232. https://doi.org/10.1016/j.polymdegradstab.2005.09.004.

Mailhot, B., Gardette, J.-L., 1994. Mechanism of poly(styrene-co-acrylonitrile) photooxidation. Polym. Degrad. Stab. 44, 237–247. https://doi.org/10.1016/0141-3910(94)90168-6.

Maris, J., Bourdon, S., Brossard, J.-M., Cauret, L., Fontaine, L., Montembault, V., 2018. Mechanical recycling: Compatibilization of mixed thermoplastic wastes. Polym.

Degrad. Stab. 147, 245–266. https://doi.org/10.1016/j.polymdegradstab.2017.11.001.
Moore, J., 1973. Acrylonitrile-butadiene-styrene (ABS) - a review. Composites 4, 118–130. https://doi.org/10.1016/0010-4361(73)90585-5.
Moustaghfir, A., Rivaton, A., Tomasella, E., Mailhot, B., Cellier, J., Jacquet, M., Gardette, J.-L., 2005. Photostabilization of polycarbonate by ZnO coatings. J. Appl. Polym. Sci. 95, 380–385. https://doi.org/10.1002/app.21316.
Noda, I., Dowrey, A.E., Haynes, J.L., Marcott, C., 2007. Group Frequency Assignments for Major Infrared Bands Observed in Common Synthetic. In: Polymers, in: Physical Properties of Polymers Handbook. Springer, New York, New York, NY, pp. 395–406. https://doi.org/10.1007/978-0-387-69002-5_22.
Oh, S.-K., Kim, W.-D., Pedrycz, W., Seo, K., 2014. Fuzzy Radial Basis Function Neural Networks with information granulation and its parallel genetic optimization. Fuzzy Sets Syst. 237, 96–117. https://doi.org/10.1016/j.fss.2013.08.011.
Piton, M., Rivaton, A., 1997. Photo-oxidation of ABS at long wavelengths (λ > 300 nm). Polym. Degrad. Stab. 55, 147–157. https://doi.org/10.1016/S0141-3910(96)00116-4.
QUV Accelerated Weathering Tester [WWW Document], n.d. . Q-LAB. URL https://www.q-lab.com/products/quv-weathering-tester/quv (accessed 2.14.19).
Rabello, M.S., White, J.R., 1997. The role of physical structure and morphology in the photodegradation behaviour of polypropylene. Polym. Degrad. Stab. 56, 55–73. https://doi.org/10.1016/S0141-3910(96)00202-9.
Ragaert, K., Delva, L., Van Geem, K., 2017. Mechanical and chemical recycling of solid plastic waste. Waste Manag. 69, 24–58. https://doi.org/10.1016/j.wasman.2017.07.044.
Rahmani, S., Pour Khalili, N., Khan, F., Hassani, S., Ghafour-Boroujerdi, E., Abdollahi, M., 2018. Bisphenol A: What lies beneath its induced diabetes and the epigenetic modulation?. Life Sci. 214, 136–144. https://doi.org/10.1016/j.lfs.2018.10.044.
Rivaton, A., 1995. Recent advances in bisphenol-A polycarbonate photodegradation. Polym. Degrad. Stab. 49, 163–179. https://doi.org/10.1016/0141-3910(95)00069-X.
Roh, S.-B., Oh, S.-K., Park, E.-K., Choi, W.Z., 2017. Identification of black plastics realized with the aid of Raman spectroscopy and fuzzy radial basis function neural networks classifier. J. Mater. Cycles Waste Manag. 19, 1093–1105. https://doi.org/10.1007/s10163-017-0620-6.
Roh, S.-B., Park, S.-B., Oh, S.-K., Park, E.-K., Choi, W.Z., 2018. Development of intelligent sorting system realized with the aid of laser-induced breakdown spectroscopy and hybrid preprocessing algorithm-based radial basis function neural networks for recycling black plastic wastes. J. Mater. Cycles Waste Manag., 1–16 https://doi.org/10.1007/s10163-018-0701-1.
Rozenstein, O., Puckrin, E., Adamowski, J., 2017. Development of a new approach based on midwave infrared spectroscopy for post-consumer black plastic waste sorting in the recycling industry. Waste Manag. 68, 38–44. https://doi.org/10.1016/j.wasman.2017.07.023.
Saviello, D., Pouyet, E., Toniolo, L., Cotte, M., Nevin, A., 2014. Synchrotron-based FTIR microspectroscopy for the mapping of photo-oxidation and additives in acrylonitrile–butadiene–styrene model samples and historical objects. Anal. Chim. Acta 843, 59–72. https://doi.org/10.1016/j.aca.2014.07.021.
Shimada, J., Kabuki, K., 1968. The mechanism of oxidative degradation of ABS resin. Part II. The mechanism of photooxidative degradation. J. Appl. Polym. Sci. 12, 671–682. https://doi.org/10.1002/app.1968.070120406.
Signoret, C., Caro-Bretelle, A.-S., Lopez-Cuesta, J.-M., Ienny, P., Perrin, D., 2019a. MIR spectral characterization of plastic to enable discrimination in an industrial recycling context: I. Specific case of styrenic polymers. Waste Manag. 95, 513–525. https://doi.org/10.1016/j.wasman.2019.05.050.
Signoret, C., Caro-Bretelle, A.-S., Lopez-Cuesta, J.-M., Ienny, P., Perrin, D., 2019b. MIR spectral characterization of plastic to enable discrimination in an industrial recycling context: II. Specific case of polyolefins. Waste Manag. 98, 160–172. https://doi.org/10.1016/j.wasman.2019.08.010.
Signoret, C., Edo, M., Lafon, D., Caro-Bretelle, A.-S., Lopez-Cuesta, J.-M., Ienny, P., Perrin, D., n.d. Degradation of styrenic plastics during recycling: Impact of reprocessing photodegraded material on aspect and mechanical properties. J. Polym. Environ. Submitted.
Silvenius, F., Grönman, K., Katajajuuri, J.-M., Soukka, R., Koivupuro, H.-K., Virtanen, Y., 2014. The Role of Household Food Waste in Comparing Environmental Impacts of Packaging Alternatives. Packag. Technol. Sci. 27, 277–292. https://doi.org/10.1002/pts.2032.
Song, D., Gao, J., Li, X., Lu, L., 2014. Evaluation of aging behavior of polypropylene in natural environment by principal component analysis. Polym. Test. 33, 131–137. https://doi.org/10.1016/j.polymertesting.2013.11.014.
Sonnenschein, M.F., 2014. Polyurethanes: Science, Technology, Markets, and Trends, Wiley Series on Polymer Engineering and Technology. John Wiley & Sons, Inc, Hoboken, NJ. https://doi.org/10.1002/9781118901274.
Thompson, R.C., Moore, C.J., vom Saal, F.S., Swan, S.H., 2009. Plastics, the environment and human health: current consensus and future trends. Philos. Trans. R. Soc. B Biol. Sci. 364, 2153–2166. https://doi.org/10.1098/rstb.2009.0053.
Vaillant, D., Lacoste, J., Dauphin, G., 1994. The oxidation mechanism of polypropylene: contribution of 13C-NMR spectroscopy. Polym. Degrad. Stab. 45, 355–360. https://doi.org/10.1016/0141-3910(94)90205-4.
Vilaplana, F., Karlsson, S., Ribes-Greus, A., Schade, C., Nestle, N., 2011. NMR relaxation reveals modifications in rubber phase dynamics during long-term degradation of high-impact polystyrene (HIPS). Polymer (Guildf). 52, 1410–1416. https://doi.org/10.1016/j.polymer.2011.02.005.
Vrancken, C., Longhurst, P.J., Wagland, S.T., 2017. Critical review of real-time methods for solid waste characterisation: Informing material recovery and fuel production. Waste Manag. 61, 40–57. https://doi.org/10.1016/j.wasman.2017.01.019.
Wang, C., Wang, H., Fu, J., Liu, Y., 2015. Flotation separation of waste plastics for recycling—A review. Waste Manag. 41, 28–38. https://doi.org/10.1016/j.wasman.2015.03.027.
Wu, G., Li, J., Xu, Z., 2013. Triboelectrostatic separation for granular plastic waste recycling: A review. Waste Manag. 33, 585–597. https://doi.org/10.1016/j.wasman.2012.10.014.
Yarsley, V.E., Couzens, E.G., 1941. Plastics. Pelican books, Allen Lane, Penguin Books.